GLACIER MAPPING FROM SENTINEL-1 SAR TIME SERIES WITH DEEP LEARNING IN SVALBARD

Konstantin A. Maslov[1], Thomas Schellenberger[2], Claudio Persello[1], Alfred Stein[1]

[1] Faculty of Geo-Information Science and Earth Observation, University of Twente, Enschede, The Netherlands
[2] Faculty of Mathematics and Natural Sciences, University of Oslo, Oslo, Norway

ABSTRACT

Glaciers are one of the essential climate variables. Tracking their areal changes over time is of high importance for monitoring the impacts of climate change and designing adaptation strategies. Mapping glaciers from optical remote sensing data might result in a very limited temporal resolution due to the absence of cloud-free imagery at the end of the ablation season. Synthetic aperture radar (SAR) solves this problem as it can operate in almost all weather conditions. Here, we present a deep learning strategy for glacier mapping based solely on Sentinel-1 SAR data in Svalbard. We test two options for integrating SAR image time series into deep learning models, namely, 3D convolutions and long short-term memory (LSTM) cells. Both proposed models achieve an intersection over union (IoU) of 0.964 on the test subset. Our results highlight the applicability of SAR data in glacier mapping with the potential to obtain glacier inventories with higher temporal resolution. We will share our codes and dataset upon acceptance.

Index Terms— Glacier mapping, Svalbard, synthetic aperture radar, deep learning, 3D convolution, long short-term memory.

1. INTRODUCTION

Glaciers are an essential climate variable, and their areal changes hold significant importance for monitoring and adaptation to climate change [1]. Their sensitivity to temperature and precipitation changes makes them crucial in understanding climate dynamics. The retreat of glaciers substantially impacts sea-level rise, alters water resources in terms of quantity and quality, influences the frequency of geohazard events and drives ecological shifts [2]. Thus, precise glacier mapping is critical for climate and environmental studies. Traditionally, optical satellite images are used to map glaciers [3, 4]. Optical images, however, are affected by clouds, thus limiting the temporal resolution of the glacier inventories in cases when, e.g., no cloud-free scenes are available at the end of the ablation season. Monitoring dynamic glacier processes like front calving and surges might also demand higher temporal resolution. Synthetic aperture radar (SAR) data has the potential to overcome these issues due to the SAR ability to penetrate clouds, acquisitions during the polar night and increased volumes of data available in recent years. SAR data has been used as additional features to support glacier mapping [4]. For instance, interferometric SAR coherence is found to be a strong predictor for glacier outlines [5]. SAR time series potential for glacier mapping was also explored qualitatively in [6]. So far, no attempt has been made to use SAR time series to train directly an end-to-end machine learning algorithm to map glacier outlines.

This study presents a deep learning strategy for regional glacier mapping in Svalbard solely from SAR time series data. We tested two options for integrating SAR scene time series into deep learning models—3D convolutions and long short-term memory (LSTM) cells. Both models achieve a very high intersection over union (IoU) of 0.964 and produce almost identical results. We also explored how the model performance changes by changing the number of acquisitions per year used for training and inference, proving that incorporating as many scenes as available is beneficial. The high accuracy of the models indicates a promising direction for further research and applications.

2. STUDY AREA AND DATA

Svalbard, a Norwegian archipelago located in the Arctic Ocean, spans approximately $62000 \, \text{km}^2$, with glaciers covering over 60% of its landmass. Observations have documented an increase in the rate of glacial melting and retreat, contributing to global sea level rise [7]. Tidewater glaciers in Svalbard are experiencing dynamic changes at their calving fronts. The frequency and magnitude of calving events further influence the rate of glacial retreat. The changes in both melting and calving dynamics provide quantitative evidence of the impact of climate warming on the Arctic region [7].

In this study, we utilized Sentinel-1A images covering almost the whole of Svalbard (except Kvitøya) from two distinct satellite stripes in the ascending orbit. Specifically, we
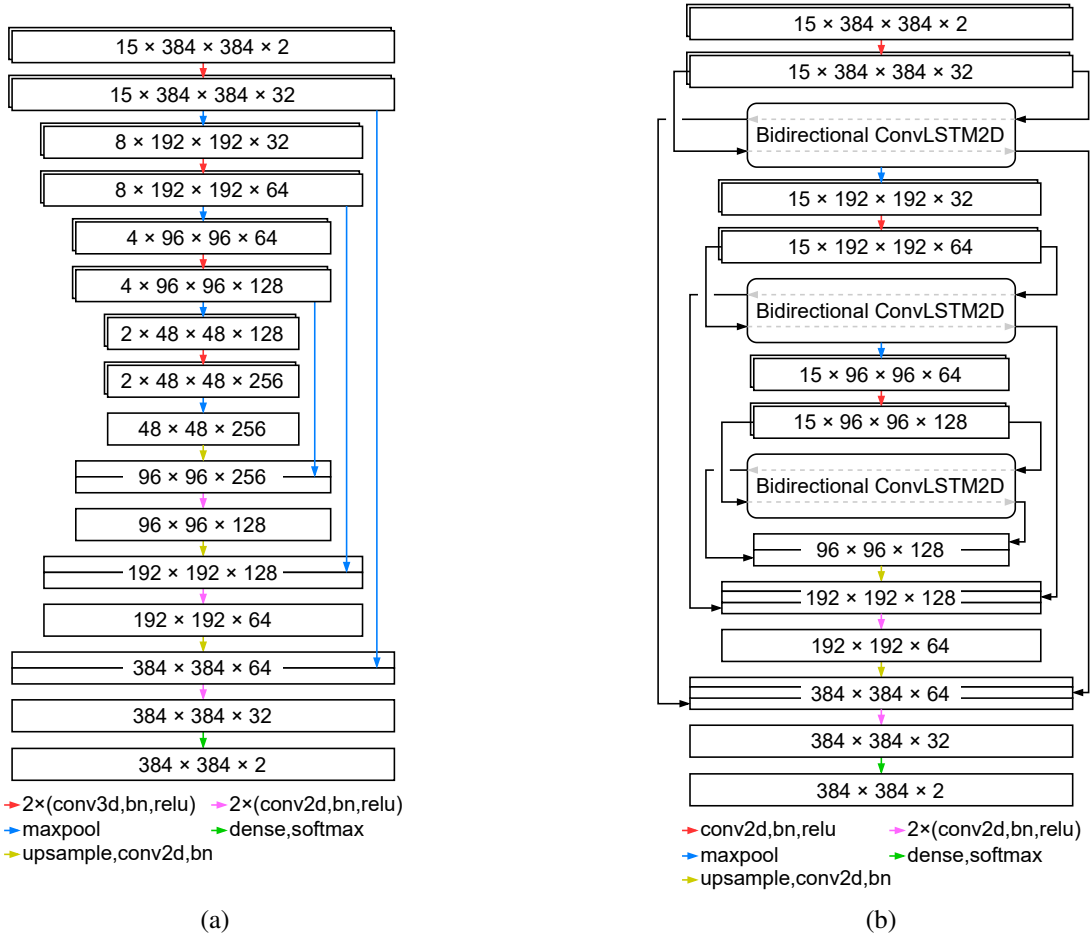
Fig. 1: The proposed deep learning models: (a) based on 3D convolutions and (b) based on LSTM. Residual connections are omitted for brevity.
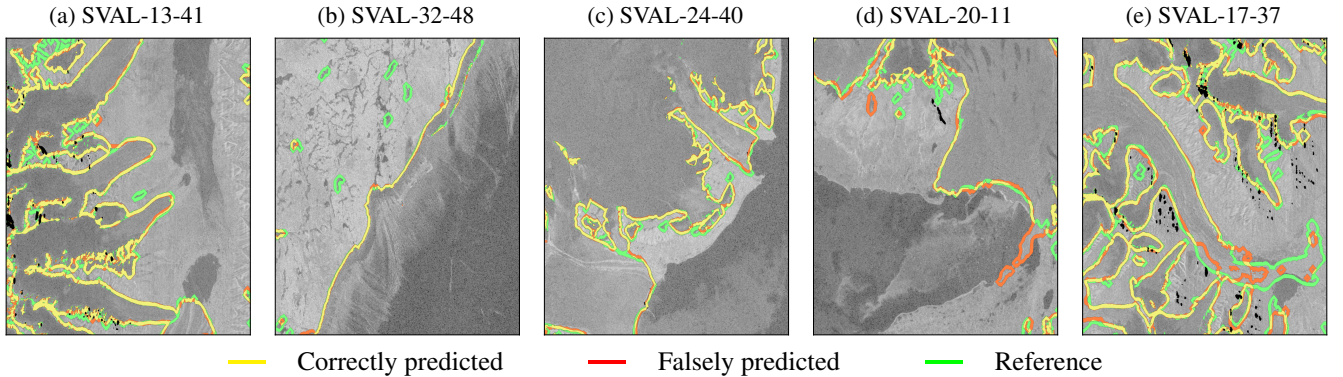
employed 15 radiometrically terrain corrected (RTC) [8] mosaics per one stripe from 2016 with a 24-day interval between acquisitions. Additionally, we incorporated interferometric coherence imagery. These interferometric coherence images were structured such that the primary images were spaced 24 days apart as well, while the secondary images were positioned at 12-day intervals forward from the primary images. The RTC data utilized in our analysis were co-polarized and provided a spatial resolution of 10 meters. The interferometric coherence data were of a coarser 40-meter resolution, later resampled to 10-meter resolution for consistency. The SAR data were obtained directly from the Alaska Satellite Facility Distributed Active Archive Center (ASF DAAC 2023, contains modified Copernicus Sentinel data 2016, processed by ESA). As reference data for training and evaluation, a Svalbard glacier inventory from 2016 and 2017 was used [9].

The whole archipelago was divided into square tiles, each measuring 10 km by 10 km. A random split allocated 60% of these tiles for training purposes, 20% for validation and the remaining 20% for testing. Tiles not covering glaciated landmass were excluded from the dataset, as well as Kvitøya

island. The dataset thus includes 438 training tiles (spanning 43800 km^2), 142 validation tiles (14200 km^2) and 142 testing tiles (14200 km^2).

3. METHODS

We utilized two straightforward ways of incorporating image time series into deep learning models. Both models follow a typical design of convolutional neural networks for semantic image segmentation such as U-Net [10]. In this case, the models take a time series of acquisitions as an input and transform it into one segmentation map that corresponds to the glacier outlines observed at the end of the ablation season. The first model (Figure 1a) is based on 3D convolutions, where time is one of the dimensions and is treated in the same way as rows and columns of the images, similar to [11]. The second model (Figure 1b) employs convolutional long short-term memory (LSTM) cells to extract temporal features as proposed in [12]. To facilitate the training process and enrich the internal feature representations, we also added residual connections [13] to both models.

(a) SVAL-13-41 (b) SVAL-32-48 (c) SVAL-24-40 (d) SVAL-20-11 (e) SVAL-17-37

— Correctly predicted   — Falsely predicted   — Reference

Fig. 2: Predictions of the 3D convolutional model. Correctly classified boundaries, false predictions and missed reference are depicted in yellow, red and green, respectively. The numbers refer to the tile positions within the grid. A Sentinel-1 image acquired at the end of the ablation season is used as a basemap. Source: ASF DAAC 2023, contains modified Copernicus Sentinel data 2016, processed by ESA.

Table 1: Comparison of the models and the number of acquisitions per year used.

Model	#acquisitions	Precision	Recall	F1-score	IoU
3D conv	1	0.822	0.941	0.877	0.781
3D conv	3	0.973	0.949	0.961	0.924
3D conv	5	0.981	0.955	0.968	0.937
3D conv	15	0.984	**0.979**	**0.982**	**0.964**
LSTM	15	**0.986**	0.976	0.982	0.964

The models were trained with randomly extracted 384×384 pixel patches. We utilized the Adam optimizer with focal loss minimization, enhanced by label smoothing. A cosine decay schedule with warm restarts was applied to the learning rate, starting at $5e^{-4}$ and spanning four cycles of 10, 20, 40, and 80 epochs. Only the top-performing models on the validation set were selected for further evaluation. We also applied on-the-fly augmentations such as random flips, rotations, cropping, rescaling, contrast adjustments, Gaussian noise, and feature occlusion by dropping out rectangular input regions.

We conducted the training and deployment of the models on cloud-based servers with NVIDIA RTXA6000 GPUs, CPUs with 16 cores and a 2.3 GHz clock speed, and 110 GB of RAM. The training duration for a single model encompassing the full dataset spanned around two weeks for the 3D convolutional model, while the LSTM-based model required about three weeks. The application of these models to the testing subset generally took several tens of minutes.

4. RESULTS

The performance metrics for both the 3D convolutional and LSTM models are presented in Table 1. The models achieved remarkably similar results, each yielding an IoU of 0.964. Any differences in their outputs are likely to be attributable to noise associated with the network weight initialization or random data sampling during training. Our analysis explored the impact of varying the total number of acquisitions on the model accuracy. We compared scenarios involving the entire-year data (15 acquisitions, 24 days apart) against subsets of just 1, 3, and 5 acquisitions, specifically chosen around the peak of the ablation season. Expectedly, an increase in the number of acquisitions corresponded to improved model performance, proving the value of incorporating comprehensive seasonal data throughout the year.

Figure 2 demonstrates the classification results of five test tiles as derived from the 3D convolutional model. We omit here the results from the LSTM model as they are almost identical and thus are not very informative. The model correctly mapped the majority of ice. It tended, however, to misclassify small glaciers and tributaries (Figure 2a–e). It correctly predicted the calving front positions in most cases (Figure 2c), but overpredictions across the coastlines were possible (Figures 2d). The model also failed to classify a considerable debris-like patch at the termini of Lisbetbreen and Universitetsbreen (Figure 2e). Notably, its inclusion has also been discussed by the creators of the inventory [9]. Furthermore, this debris-covered patch was not included in both the Randolph Glacier Inventory (2010 data) [14] and a later inventory from the Norwegian Polar Institute (2020, preliminary version obtained from the authors) [15], which highlights the complexity of this specific target and may point to ambiguities in the reference data utilized in our study or other inventories.

5. CONCLUSION

This study showcased the effectiveness of deep learning models using SAR time series data for mapping glaciers in Svalbard, achieving a high IoU of 0.964. The study confirmed that more SAR acquisitions lead to better model accuracy as compared to just a few acquisitions during the transition from the ablation to the accumulation season. The optimal choice of

acquisition dates, however, remains an open question. For instance, one could explore utilizing fewer acquisitions sparsely scattered across a year or even denser time series. While the models reliably mapped larger glaciers, they were less successful with smaller glaciers, indicating room for improvement. The inconsistencies noted between the model predictions and existing glacier inventories highlight the potential for SAR-based models to update and refine existing glacier inventories. Further research could enhance model precision and explore the combination of SAR with other data sources such as digital elevation models or optical sensors for comprehensive glacier monitoring. In addition, implementing the same strategy for other areas is crucial to confirm its adaptability and readiness for operational use.

ACKNOWLEDGEMENTS

REFERENCES

[1] World Meteorological Organization, United Nations Environment Programme, International Science Council & Intergovernmental Oceanographic Commission of the United Nations Educational, Scientific and Cultural Organization, "The 2022 gcos ecvs requirements (gcos 245)," 2022.

[2] R. Hock, G. Rasul, C. Adler, B. Cáceres, S. Gruber, Y. Hirabayashi, M. Jackson, A. Kääb, S. Kang, S. Kutuzov, Al. Milner, U. Molau, S. Morin, B. Orlove, and H. Steltzer, "High mountain areas," *IPCC Special Report on the Ocean and Cryosphere in a Changing Climate*, pp. 131–202, 2019.

[3] F. Paul, S. H. Winsvold, A. Kääb, T. Nagler, and G. Schwaizer, "Glacier remote sensing using sentinel-2. part ii: Mapping glacier extents and surface facies, and comparison to landsat 8," *Remote Sensing*, vol. 8, 7 2016.

[4] K. A. Maslov, C. Persello, T. Schellenberger, and A. Stein, "Glavitu: A hybrid cnn-transformer for multi-regional glacier mapping from multi-source data," in *IGARSS 2023 - 2023 IEEE International Geoscience and Remote Sensing Symposium*, 2023, pp. 1233–1236.

[5] Stefan Lippl, Saurabh Vijay, and Matthias Braun, "Automatic delineation of debris-covered glaciers using insar coherence derived from x-, c- and l-band radar data: A case study of yazgyl glacier," *Journal of Glaciology*, vol. 64, pp. 811–821, 10 2018.

[6] B. Zhang, G. Liu, X. Wang, Y. Fu, Q. Liu, B. Yu, R. Zhang, and Z. Li, "Semi-automated mapping of complex-terrain mountain glaciers by integrating l-band sar amplitude and interferometric coherence," *Remote Sensing 2022, Vol. 14, Page 1993*, vol. 14, pp. 1993, 4 2022.

[7] T. V. Schuler, J. Kohler, N. Elagina, J. O. M. Hagen, A. J. Hodson, J. A. Jania, A. M. Kääb, B. Luks, J. Małecki, G. Moholdt, V. A. Pohjola, I. Sobota, and W. J. J. Van Pelt, "Reconciling svalbard glacier mass balance," *Frontiers in Earth Science*, vol. 8, 5 2020.

[8] O. Frey, M. Santoro, C. L. Werner, and U. Wegmuller, "Dem-based sar pixel-area estimation for enhanced geocoding refinement and radiometric normalization," *IEEE Geoscience and Remote Sensing Letters*, vol. 10, no. 1, pp. 48–52, 2013.

[9] F. Paul, F. Goerlich, and P. Rastner, "A new glacier inventory for svalbard from sentinel-2 and landsat 8 for improved calculation of climate change impacts," in *EGU General Assembly*, 2021, online, 19–30 Apr 2021, EGU21-14499.

[10] O. Ronneberger, P. Fischer, and T. Brox, "U-net: Convolutional networks for biomedical image segmentation," *Lecture Notes in Computer Science (including subseries Lecture Notes in Artificial Intelligence and Lecture Notes in Bioinformatics)*, vol. 9351, pp. 234–241, 5 2015.

[11] D. Tran, L. Bourdev, R. Fergus, L. Torresani, and M. Paluri, "Learning spatiotemporal features with 3d convolutional networks," in *Proceedings of the IEEE International Conference on Computer Vision (ICCV)*, December 2015.

[12] X. Shi, Z. Chen, H. Wang, D. Y.n Yeung, W. K. Wong, and W. C. Woo, "Convolutional lstm network: A machine learning approach for precipitation nowcasting," *Advances in Neural Information Processing Systems*, vol. 2015-January, pp. 802–810, 6 2015.

[13] K. He, X. Zhang, S. Ren, and J. Sun, "Deep residual learning for image recognition," in *Proceedings of the IEEE Computer Society Conference on Computer Vision and Pattern Recognition*. 12 2015, vol. 2016-December, pp. 770–778, IEEE Computer Society.

[14] RGI Consortium, "Randolph glacier inventory—a dataset of global glacier outlines, version 6.," *Boulder, Colorado USA. NSIDC: National Snow and Ice Data Center.*, 2017.

[15] Aniek Lith, Geir Moholdt, and Jack Kohler, "Svalbard glacier inventory based on sentinel-2 imagery from summer 2020," 2021.